

# Mean magnetic field and energy balance of Parker's surface-wave dynamo

A.J.H. Ossendrijver and P. Hoyng

SRON Laboratorium voor Ruimteonderzoek, Sorbonnelaan 2, 3584 CA Utrecht, The Netherlands

Received 22 April 1996 / Accepted 24 January 1997

**Abstract.** We study the surface-wave dynamo proposed by Parker (1993) as a model for the solar dynamo, by solving equations for the mean magnetic field  $\mathbf{B}_0$ , as well as for the mean 'magnetic energy tensor'  $\mathbf{T} = \langle \mathbf{B}\mathbf{B} \rangle / 8\pi$ . This tensor provides information about the energy balance, rms field strengths and correlation coefficients between field components. The main goal of this paper is to check whether the equations for  $\mathbf{B}_0$  and  $\mathbf{T}$  are compatible, i.e. whether both have "reasonable" solutions for a set of "reasonable" parameters. We apply the following constraints:  $\mathbf{B}_0$  has a period of 22 years and, taking into account the effect of period variations, a decay time of 10 dynamo periods, and  $\mathbf{T}$  is marginally stable. We find that under these constraints, the equations for  $\mathbf{B}_0$  and  $\mathbf{T}$  are compatible only if, apart from turbulent transport out of the dynamo region, an additional energy sink is introduced. If this extra term is omitted, then marginal stability of  $\mathbf{T}$  requires a turbulent diffusion in the convection zone of the order  $\beta_2 \gtrsim 3 \times 10^{14} \text{ cm}^2 \text{ s}^{-1}$ , whereas the conditions on  $\mathbf{B}_0$  require  $\beta_2 \approx 10^{12} \text{ cm}^2 \text{ s}^{-1}$ . Furthermore, the rms surface field strength, the maximum rms field strength and the magnetic energy flux through the upper surface of the convection zone cannot simultaneously assume solar values. We explore the possibility that the extra energy sink is provided by resistive dissipation, hitherto not accounted for in the equation for  $\mathbf{T}$ , by considering various cases. We demonstrate that with a heuristically modified equation for  $\mathbf{T}$ , the inconsistencies can be removed. Our results suggest that resistive dissipation is the dominant sink of magnetic energy, and that resistive heating may amount to several percent of the solar luminosity.

**Key words:** Sun: magnetic fields – MHD – turbulence

## 1. Introduction

In recent years observational evidence and various calculations have resulted in a coherent set of requirements for solar-dynamo models. From measurements of the emerging flux in active regions it is inferred that the total subsurface flux is of the order  $10^{24} \text{ Mx}$  (Galloway & Weiss 1981; Golub et al. 1981). This

amount of flux cannot be maintained in the convection zone, because buoyancy forces would lead to rapid expulsion on a timescale of months, much shorter than the timescale for the amplification of toroidal field by a radial velocity shear.

Van Geffen & Hoyng (1993) and Van Geffen (1993a, 1993b) have confirmed that a dynamo operating within the convection zone cannot be responsible for the solar cycle. These authors found that the field strength at the base of the convection zone is only of order  $B_{\text{rms}} \approx 200 \text{ G}$  and that the mean field  $\mathbf{B}_0$  decays on a timescale of about 2 weeks due to phase mixing (this concept is explained below). A convection zone dynamo thus produces only a weak, rapidly fluctuating aperiodic field.

It is currently believed that the magnetic flux is concentrated in the stably stratified overshoot layer between the radiative core and the convection zone (Zwaan 1978, Spiegel & Weiss 1980). In this layer, which has a thickness of about  $2 \times 10^9 \text{ cm}$ , the field must be of order  $2 \times 10^4 \text{ G}$  to explain the measured flux. Since not all the flux in the overshoot layer may emerge at the surface, and the field may have a filamentary structure, the actual field strength may be of order  $10^5 \text{ G}$ . It has been shown that such strong fields can indeed be stored in the overshoot layer (e.g. van Ballegooijen 1982, Moreno-Insertis et al. 1992). A value of  $10^5 \text{ G}$  is also in agreement with the field strength required for rising flux tubes to resist the Coriolis force sufficiently so that they emerge at the solar surface within the observed activity belts and having the correct tilt with respect to the equator (Choudhuri 1989, D'Silva & Choudhuri 1993, Caligari et al. 1995).

The evolution of the mean magnetic field  $\mathbf{B}_0$  is described by the following equation:

$$\partial_t \mathbf{B}_0 = \nabla \times \{ \mathbf{u}_0 \times \mathbf{B}_0 + \alpha \mathbf{B}_0 - \beta \nabla \times \mathbf{B}_0 \}. \quad (1)$$

Here  $\mathbf{u}_0 = \Omega r \sin \theta \mathbf{e}_\phi$  is the large scale velocity field. Helioseismological data indicate that the Sun rotates differentially and that the radial velocity shear is concentrated near the base of the convection zone. Hence strong azimuthal fields in the overshoot layer can be produced by differential rotation. The sign of  $\partial\Omega/\partial r$  is positive at low latitudes and negative at high latitudes (Goode 1995). If  $\mathbf{u}_1$  denotes the turbulent velocity field and if

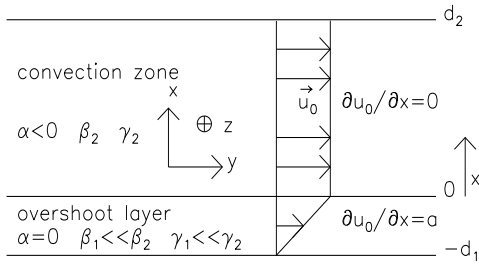


**Fig. 1.** Geometry of Parker's interface wave dynamo. In our calculations we adopted  $d_1 = 2 \times 10^9$  cm,  $d_2 = 2 \times 10^{10}$  cm and  $a = 4 \times 10^{-6}$  s $^{-1}$ .

$\tau_c$  is the typical correlation time of the turbulence, we may write  $\alpha$  and the turbulent diffusivity  $\beta$  as

$$\alpha = -\frac{1}{3}\tau_c \langle \mathbf{u}_1 \cdot (\nabla \times \mathbf{u}_1) \rangle, \quad \beta = \frac{1}{3}\tau_c \langle u_1^2 \rangle. \quad (2)$$

Thus  $\alpha$  is proportional to the mean helicity of the turbulent velocity field. This quantity is nonzero in a rotating turbulent medium such as the solar convection zone. Since, in the Northern hemisphere,  $\alpha$  is believed to be positive in the bulk of the convection zone and to change its sign near the base,  $\alpha \partial \Omega / \partial r$  probably has the right sign in the lower part of the convection zone for dynamo waves to travel towards the equator at low latitudes. Due to the high field strength in the overshoot layer, well above the equipartition value,  $\alpha$  and  $\beta$  are assumed to be greatly reduced compared to their values in the convection zone.

It was suggested by Parker (1993) that such an overshoot-layer dynamo can be modelled through spatial separation of the radial velocity shear and the  $\alpha$ -effect. The model proposed by Parker employs a flat geometry, and, in our case, has local validity in the Northern hemisphere of the Sun (Fig. 1). It describes a convection zone (region 2) in which  $\alpha \neq 0$  and the velocity shear is zero, below which there is a thin overshoot layer (region 1). Here  $\alpha = 0$ , and the turbulent diffusivity is reduced, i.e.

$$f_\beta = \frac{\beta_1}{\beta_2} \ll 1. \quad (3)$$

One has to allow for some turbulent diffusion in the overshoot layer, because dynamo action requires transport between the two regions. Differential rotation is schematically described by

$$\mathbf{u}_0(x) = u_0(x)\mathbf{e}_y, \quad \partial_x u_0 = \begin{cases} a & (-d_1 < x < 0) \\ 0 & (0 < x < d_2). \end{cases} \quad (4)$$

Cartesian coordinates are employed, with  $x$  denoting the radial,  $y$  the azimuthal and  $z$  the latitudinal coordinate. The interface between the overshoot layer and the convection zone is at  $x = 0$ ; the equator is at  $z = 0$ . We assume translational symmetry along the  $y$ -axis and consider only axisymmetric solutions ( $\partial/\partial y = 0$ ). The geometry of the model differs from Parker's original model in that boundaries are specified at  $x = -d_1$  and  $x = d_2$ . The introduction of boundaries is necessary for computing the energy balance of the dynamo, in particular the energy loss into

empty space (Sect. 4.2). For the sake of consistency, we solve the equation for  $\mathbf{B}_0$  using the same geometry. The effect of the boundaries on  $\mathbf{B}_0$  is expected to be small, since the dynamo operates at the interface between overshoot layer and convection zone.

Our approach to mean-field dynamo theory is statistical and is based on the 'finite-energy method' (Hoyng 1987, Van Geffen & Hoyng 1993, Van Geffen 1993a), which can be briefly described as follows. If the parameters  $\alpha$  and  $\beta$  are taken as non-fluctuating constants, as is usually done, Eq. (1) applies strictly only for a mean field that is defined as an ensemble average. Every ensemble member represents a dynamo that is on average marginally stable with, in the solar case, a mean period  $P_{\text{dyn}} = 22$  years and, on top of that, period fluctuations of the order  $\Delta P_{\text{dyn}}/P_{\text{dyn}} \approx 0.1$ . If we ignore for the moment latitude dependence, amplitude modulations and other details of the solar cycle, we may schematically represent the magnetic field of one ensemble member as  $\mathbf{B} \propto \cos(\omega t + \psi_0)$ , where  $\omega = 2\pi/P_{\text{dyn}}$  is the dynamo frequency, subject to variations ( $\delta\omega/\omega \approx 0.1$ ), and  $\psi_0$  is an initial phase. The frequency variations give rise to phase mixing between the ensemble members, so that the resulting *mean* field is slightly subcritical, decaying at a rate  $|\gamma| \approx 0.1/P_{\text{dyn}}$ . The decay time  $\tau_{\text{dec}} = 1/|\gamma|$  is interpreted as the coherence time of the *actual* magnetic field.

The result of phase mixing is different, however, for the magnetic energy density  $|\mathbf{B}|^2/8\pi$ , since it is positive definite. For each ensemble member we may approximate  $B^2 \propto \cos^2(\omega t + \psi_0) = \frac{1}{2} + \frac{1}{2}\cos 2(\omega t + \psi_0)$ . Thus the magnetic energy of a periodic dynamo has a constant term, and an oscillating term. Applying the ensemble average to  $B^2$ , we infer that the fundamental mode of  $\langle B^2 \rangle$  should be (roughly) constant and non-periodic. The periodic overtones, which result from the oscillating part of  $B^2$ , should decay due to phase mixing.

To summarise, the finite-energy method provides us with the following constraints: the mean magnetic energy is marginally stable and non-oscillatory and, in the solar case, the mean magnetic field has a period of 22 years and a decay time of about 10 dynamo periods.

The main goal of the present paper is to verify whether these constraints can be met. The motivation for using Parker's model came from the intuitive feeling that here the decay time of the mean field may be of the right order, much longer than that of a convection-zone dynamo (Van Geffen & Hoyng 1993 and Van Geffen 1993a), because the overshoot layer, where strong fields are produced, has a lower level of turbulence, hence maybe also less variability and less phase mixing. Van Geffen (1993b) found that the mean-field decay time did not increase significantly when a lower turbulent diffusivity is adopted near the base of the convection zone. However, since his calculations were carried out on a finite grid and his spatial resolution in the overshoot layer was insufficient, he was not able to treat large discontinuities. The simplified geometry employed in the present paper allows us to obtain analytical expressions for the mean field and the mean magnetic energy on both sides of the interface between the overshoot layer and the convection zone.

Since no closed equation exists for  $\langle B^2 \rangle$ , it is necessary to consider an equation for

$$\mathbb{T} = \langle \mathbf{B}\mathbf{B} \rangle / 8\pi, \quad (5)$$

henceforth referred to as the *mean magnetic energy tensor*. Our main conclusion is that, also for Parker's surface dynamo wave, the constraints posed by the finite-energy method cannot be met for reasonable parameters, unless the equation for  $\mathbb{T}$ , as introduced by Knobloch (1978) and Hoyng (1987), is modified by including an additional energy sink. Such a modification is introduced and motivated in Sect. 2. In Sect. 3 we turn to the mean magnetic field. In Sect. 4 we present the equations, boundary conditions and main assumptions for  $\mathbb{T}$ . In the following three sections we treat three cases, each based on a different assumption for the resistive dissipation. Sect. 8 contains a discussion of our results as well as our conclusions.

## 2. Mean-field dynamo theory and resistive dissipation

The evolution of the magnetic field is described by the induction equation,

$$\partial_t \mathbf{B} = \nabla \times \{ \mathbf{u} \times \mathbf{B} - \eta \nabla \times \mathbf{B} \}. \quad (6)$$

In the solar convection zone, the velocity field  $\mathbf{u}$  has a large-scale component  $\mathbf{u}_0$ , which is more or less constant in time, and a rapidly varying turbulent component  $\mathbf{u}_1$ . This suggests that in the kinematic limit Eq. (6) can be treated as a linear stochastic differential equation with a multiplicative driving term  $\mathbf{u}_1$ . Under certain assumptions, the theory of stochastic differential equations (see for instance Van Kampen 1992) provides an equation for  $\mathbf{B}_0 = \langle \mathbf{B} \rangle$ . Here it suffice to mention that for a stochastic differential equation of the form

$$\partial_t \mathbf{A} = [L_0 + L_1] \mathbf{A}, \quad (7)$$

where  $L_0$  is a time-independent operator and  $L_1$  is a stochastic operator with  $\langle L_1 \rangle = 0$ , one obtains

$$\partial_t \langle \mathbf{A} \rangle = [L_0 + \int_0^\infty ds \langle L_1(t) L_1(t-s) \rangle] \langle \mathbf{A} \rangle. \quad (8)$$

This is a general result, valid if the correlation time  $\tau_c$  of the stochastic operator is sufficiently short ( $\tau_c |L_1| \ll 1$  and  $\tau_c |L_0| \ll 1$ ). In the case of the induction equation (6), the term containing  $\mathbf{u}_1$  is identified as  $L_1$  and the other terms (including the dissipative term) form  $L_0$ . Hence the former condition is equivalent to  $\tau_c u_1 / l \ll 1$ , which is questionable for the Sun, but we ignore this well-known problem of mean-field electrodynamics for the moment. A derivation of the mean-field equation (1) based on this method is presented e.g. by Hoyng (1992). In principle the same procedure can be applied to the magnetic energy tensor  $\mathbf{B}\mathbf{B}/8\pi$ , which obeys the following equation, obtained from Eq. (6) by adding  $B_i \partial_t B_j$  to  $B_j \partial_t B_i$ :

$$\begin{aligned} (\partial_t + \mathbf{u} \cdot \nabla) B_i B_j &= \sum_k \{ (\nabla_k u_i) B_k B_j + (\nabla_k u_j) B_k B_i \} \\ &+ \eta \nabla^2 B_i B_j - 2\eta \sum_k (\nabla_k B_i) (\nabla_k B_j). \end{aligned} \quad (9)$$

Unfortunately, this equation cannot be treated in the same manner as the induction equation itself. In the present form it is not a closed equation for  $\mathbf{B}\mathbf{B}$ , i.e. it cannot be written as  $\partial_t \mathbf{B}\mathbf{B} = L \mathbf{B}\mathbf{B}$  for some differential operator  $L$ . The closure problem is caused by the term  $-2\eta \sum_k (\nabla_k B_i) (\nabla_k B_j)$ . One manner in which this difficulty has been resolved is to ignore resistive dissipation altogether, assuming that it plays no role in the energy balance of the dynamo. In that case, a closed equation is obtained for the magnetic energy tensor, and the same method, used in deriving the mean-field equation can be applied (Knobloch 1978, Hoyng 1987).

However, solutions of this approximative equation turn out to be problematic. The core of the problem is that the only energy sink available to the dynamo is the energy flux through the upper surface of the convection zone. Marginal stability of the energy can then be realised only by making the energy transport through the dynamo by means of turbulent diffusion sufficiently effective, which in practice means that turbulent diffusivity has to be unphysically large. We demonstrate this in Sect. 5.

Resistive dissipation provides an additional energy sink, and operates through a cascade from large scales to small scales, where the field is dissipated. However, the closure problem indicates that, unlike for the mean-field equation, where it suffices to define a total diffusivity  $\beta + \eta$ , no simple recipe is available for modifying the mean-energy equation to take into account resistive dissipation. This fundamental difference between  $\mathbf{B}_0$  and  $\mathbb{T}$  originates in the different treatment of small-scale fields. The former gives a description of only the largest scales in the dynamo, since the rapidly varying small-scale fields cancel out in the averaging procedure. The latter contains all length scales, as can be seen by writing  $\mathbf{B} = \mathbf{B}_0 + \delta \mathbf{B}$ , which provides

$$\langle B^2 \rangle = B_0^2 + \langle (\delta B)^2 \rangle. \quad (10)$$

Hence resistive dissipation does not affect  $\mathbf{B}_0$ , but can be very important for  $\mathbb{T}$ .

In this paper an attempt is made to treat the effect of resistivity on  $\mathbb{T}$  in a heuristic and approximative way. For turbulent fluids with high Reynolds numbers the energy distribution over the length scales is characterised by the inertial-range spectrum, defined by (see for instance Moffatt 1978, Ch. 11 or Biskamp 1993, Ch. 7):

$$l_d \ll l \ll l_{in}. \quad (11)$$

Three different length scales can thus be distinguished:

1. a large injection length scale  $l_{in} \approx d_2$  related to variations of the mean field and the mean energy;
2. the inertial-range length scales  $l$ , related to the stretching and folding of field lines due to the turbulent velocity;
3. the dissipative length scale  $l_d$ . By definition, this is the length scale at which the dissipative timescale equals the energy-transfer timescale.

For stationary turbulence, conservation of energy implies that the injection rate, the transfer rate and the dissipation rate of the

magnetic energy are equal. Hence, in an equilibrium situation, resistive dissipation should balance the energy production, and this is achieved by continuing the energy cascade down to whatever length scale is required to balance the input. This suggests the following simple approximation: we replace the last term of Eq. (9) by a scale-independent term  $-2\nu B_i B_j$ , and we omit the term  $\eta \nabla^2 B_i B_j$ , since it will give rise to a negligible term after averaging (similar to the treatment of resistive dissipation in the equation for  $B_0$ ). The value of the dissipation coefficient  $\nu$  is dictated by the energy production rate. It is not expected that this term can describe the effect of resistive dissipation in detail, but it should account for its average effect on  $T$ . This approximation resolves the closure problem and enables us to study if resistive dissipation can, in principle, solve the inconsistencies that we encounter when it is ignored. The resulting equation for  $B_i B_j$  can be averaged using the standard methods:

$$\partial_t B_i B_j = \sum_{kl} [L_{ijkl}^{(0)} + L_{ijkl}^{(1)}] B_k B_l, \quad (12)$$

with

$$L_{ijkl}^{(0)} = (\nabla_k u_{0i}) \delta_{jl} + (\nabla_k u_{0j}) \delta_{ik} - \delta_{ik} \delta_{jl} (\mathbf{u}_0 \cdot \nabla + 2\nu), \quad (13)$$

$$L_{ijkl}^{(1)} = (\nabla_k u_{1i}) \delta_{jl} + (\nabla_k u_{1j}) \delta_{ik} - \delta_{ik} \delta_{jl} \mathbf{u}_1 \cdot \nabla. \quad (14)$$

For details on the various steps that are involved in applying Eq. (8) to Eq. (12), the reader is referred to Hoyng (1987).

### 3. The mean magnetic field

In this section our main goal is to find sets of parameters for which the mean magnetic field has a period of 22 years and a decay time of 10 dynamo periods.

#### 3.1. Equations

We express  $B_0$  in terms of the toroidal field  $T$  and the poloidal vector potential  $P$ , i.e.  $B_0 = T e_y + \nabla \times P e_y$ . Substitution into Eq. (1) gives

$$\left. \begin{aligned} (\partial_t - \beta_1 \nabla^2) P &= 0 \\ (\partial_t - \beta_1 \nabla^2) T &= -\alpha \partial_z P \end{aligned} \right\} \quad (-d_1 \leq x \leq 0), \quad (15)$$

$$\left. \begin{aligned} (\partial_t - \beta_2 \nabla^2) P &= \alpha T \\ (\partial_t - \beta_2 \nabla^2) T &= 0 \end{aligned} \right\} \quad (0 < x \leq d_2).$$

On the right hand side of the last equation, the term  $-\alpha \nabla^2 P$  has been neglected, in accordance with the  $\alpha\omega$ -approximation.

#### 3.2. Boundary conditions

We specify boundary conditions at each of the three interfaces, beginning with the one between the radiative core and the overshoot layer. Turbulent diffusivity vanishes in the radiative core.

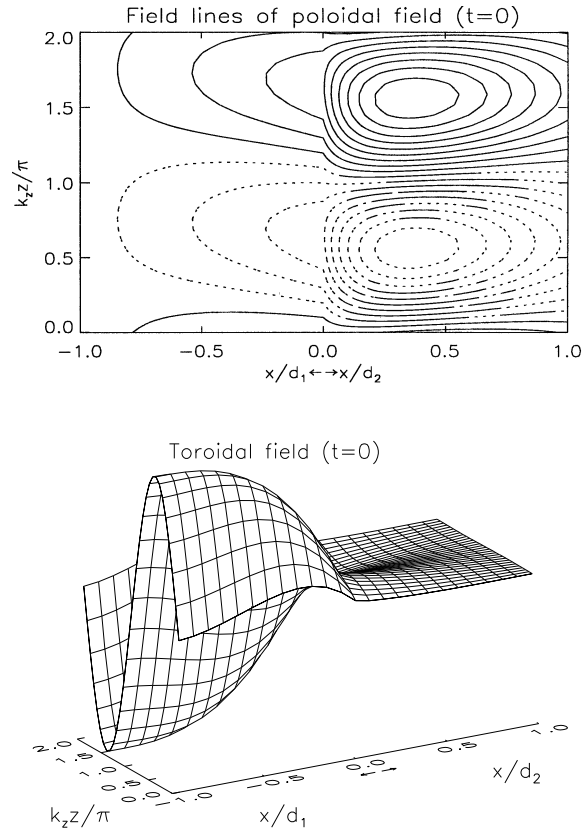


**Fig. 2.** The mean magnetic field  $B_0$  with  $\alpha = -150 \text{ cm s}^{-1}$ ,  $\beta_1 = 1.72 \times 10^{10} \text{ cm}^2 \text{ s}^{-1}$ ,  $\beta_2 = 1.55 \times 10^{12} \text{ cm}^2 \text{ s}^{-1}$ ,  $P_{\text{dyn}} = 22$  years and  $\tau_{\text{dec}} = 220$  years. The mean field is concentrated in 'belts' of alternating polarity migrating toward the equator (downwards in the figure). Top: poloidal field lines of  $B_0$  as a function of  $x$  and  $z$  at  $t = 0$ . Drawn field lines have clockwise, dashed field lines anticlockwise orientation. Poloidal field is created only in the convection zone, and diffuses into the overshoot layer. This diffusion, in combination with the migration of the dynamo wave along the  $z$ -axis, results in a phase lag that increases with the distance to the interface  $x = 0$ . Bottom: toroidal (azimuthal) field  $T$  as a function of  $x$  and  $z$  at  $t = 0$ .

Therefore no poloidal field or magnetic flux may penetrate below  $x = -d_1$  (see also Choudhuri 1990). This results in

$$P = \partial_x T = 0 \quad \text{at } x = -d_1. \quad (16)$$

At the interface between regions 1 and 2 continuity of  $B_0$  is required, i.e.

$$[[P]] = [[T]] = [[\partial_x P]] = 0 \quad \text{at } x = 0. \quad (17)$$

Here  $[[\cdot]]$  denotes the jump at the boundary. Furthermore, if we integrate the toroidal component of Eq. (1) from  $x = -\delta$  to  $x = \delta$  and let  $\delta \downarrow 0$  we obtain:

$$[[\beta \partial_x T]] = 0 \quad \text{at } x = 0, \quad (18)$$

where  $\beta$  assumes the value  $\beta_1$  for  $x = 0^-$  and  $\beta_2$  for  $x = 0^+$ . Boundary conditions at  $x = d_2$  are provided by matching the field in the convection zone to a potential field above the solar

surface (Krause & Rädler 1980). The potential field satisfies  $\nabla \times \mathbf{B}_0 = 0$ , i.e.

$$\nabla^2 P = 0; \quad \nabla \times T \mathbf{e}_y = 0 \quad (x > d_2). \quad (19)$$

Continuity of  $\mathbf{B}_0$  implies

$$\llbracket P \rrbracket = \llbracket T \rrbracket = \llbracket \partial_x P \rrbracket = 0 \quad \text{at } x = d_2. \quad (20)$$

We consider only plane-wave solutions of the form  $P = p(x)e^{ik_z z + \lambda t}$ , and similarly for  $T$  (Sect. 3.3). We use this to simplify the boundary conditions at  $x = d_2$ . First we note that Eq. (19) reduces to

$$(\partial_x^2 - k_z^2)P = 0; \quad T = 0 \quad (x > d_2). \quad (21)$$

The relevant solution for  $x > d_2$  decays exponentially with the distance to the solar surface, i.e.  $p \propto e^{-k_z(x-d_2)}$ . Hereby one of the boundary conditions (20) can be eliminated, and the remaining two may be written as follows:

$$(\partial_x + k_z)P = 0; \quad T = 0 \quad \text{at } x = d_2. \quad (22)$$

### 3.3. Solutions

We consider plane-wave solutions that propagate towards the equator along the  $z$ -axis, i.e.

$$P = p(x)e^{ik_z z + \lambda t}, \quad (23)$$

$$T = q(x)e^{ik_z z + \lambda t}. \quad (24)$$

Here  $k_z$  is the latitudinal wavevector, and the (complex) growth rate  $\lambda$  is written as

$$\lambda = i\omega + \gamma, \quad (25)$$

from which we obtain the dynamo period and the mean-field decay time,

$$P_{\text{dyn}} = 2\pi/\omega; \quad \tau_{\text{dec}} = 1/|\gamma|. \quad (26)$$

The general solution of Eq. (15) is as follows:

$$p_1/d_1 = A_1 e^{\kappa_1 x} + B_1 e^{-\kappa_1 x}, \quad (27)$$

$$q_1 = A_2 e^{\kappa_1 x} + B_2 e^{-\kappa_1 x} \quad (28)$$

$$+ \frac{iad_1 k_z x}{2\beta_1 \kappa_1} (A_1 e^{\kappa_1 x} - B_1 e^{-\kappa_1 x}), \quad (29)$$

$$p_2/d_2 = A_3 e^{\kappa_2 x} + B_3 e^{-\kappa_2 x} - \frac{\alpha x}{2\beta_2 \kappa_2 d_2} (A_4 e^{\kappa_2 x} - B_4 e^{-\kappa_2 x}), \quad (30)$$

$$q_2 = A_4 e^{\kappa_2 x} + B_4 e^{-\kappa_2 x}. \quad (31)$$

Here the indices on  $p$  and  $q$  specify the two dynamo regions, and

$$\kappa_1 = \sqrt{k_z^2 + \lambda/\beta_1}; \quad \kappa_2 = \sqrt{k_z^2 + \lambda/\beta_2}. \quad (32)$$

It is assumed that  $\text{Re } \kappa_1 > 0$  and  $\text{Re } \kappa_2 > 0$ . We have included  $d_1$  and  $d_2$  in the definition of  $p_1$  and  $p_2$  respectively, so that all the integration constants  $A_1, A_2, \dots, B_4$  have the same dimension.

On imposing the boundary conditions, we obtain eight relations between the integration constants, which are presented in Appendix A. They form a square matrix of coefficients, whose determinant should vanish. This results in a transcendental dispersion relation, every root  $\lambda_i$  of which corresponds to a dynamo mode. We are interested only in the fundamental mode, i.e. the one with the largest growth rate  $\gamma_i$ .

Since the dispersion relation cannot be solved analytically, we resort to an iterative numerical method. A useful initial value  $\lambda_0$  for the iterations is obtained from a simplified form of the dispersion relation. To that purpose we ignore all terms that grow exponentially with  $|x|$ , i.e.  $B_1 = B_2 = A_3 = A_4 = 0$ . The dispersion relation then is

$$\kappa_1 \kappa_2 (\kappa_1 + \kappa_2) (f_\beta \kappa_1 + \kappa_2) = -i\alpha k_z / 4\beta_2^2, \quad (33)$$

which corresponds to Eq. (22) of Parker (1993). Second, we use  $f_\beta \ll 1$  and approximate  $|\kappa_1| \approx \sqrt{|\lambda_0|/\beta_1} \gg |\kappa_2|$  (Eq. 32; see below for a justification). This yields

$$\kappa_1^2 \kappa_2^2 = -iC/4, \quad (34)$$

where the dynamo number  $C$  is defined as

$$C \equiv \frac{\beta_1 \alpha a}{\beta_2^3 k_z^3}. \quad (35)$$

Inserting  $\kappa_1$  and  $\kappa_2$ , it follows that

$$\lambda_0^2 + \beta_2 k_z^2 \lambda_0 + i\beta_2^2 k_z^4 C/4 = 0. \quad (36)$$

We conclude that, to first approximation, the fastest growing solution has a frequency  $\omega_0$  and a growth rate  $\gamma_0$  given by

$$\omega_0/\beta_2 k_z^2 = \frac{1}{2\sqrt{2}} \left\{ -1 + \sqrt{1 + C^2} \right\}^{1/2}, \quad (37)$$

$$\gamma_0/\beta_2 k_z^2 = -\frac{1}{2} + \frac{1}{2\sqrt{2}} \left\{ 1 + \sqrt{1 + C^2} \right\}^{1/2}. \quad (38)$$

These estimates are used as starting values for solving the exact dispersion relation iteratively.

### 3.4. Parameters

From helioseismological measurements (Goode 1995) the total velocity jump at the base of the convection zone, near the equator, is estimated to be  $ad_1 = 8 \times 10^3 \text{ cm s}^{-1}$ , so that  $a = 4 \times 10^{-6} \text{ s}^{-1}$  for  $d_1 = 2 \times 10^9 \text{ cm}$ . This supposes that the entire velocity jump occurs within the overshoot layer.

For the wavenumber in the azimuthal direction we take  $k_z = 10^{-10} \text{ cm}^{-1}$ , which corresponds to a half wavelength of  $\pi/k_z \approx 3.1 \times 10^{10} \text{ cm}$  or  $180^\circ/k_z R_\odot \approx 26^\circ$ . Thus  $|\lambda|/\beta_2 \approx \omega_\odot/\beta_2 \approx 10^{-20}$  has the same order of magnitude as  $k_z^2$ , and  $|\lambda|/\beta_1 \gg k_z^2$ . This justifies the approximation that we adopted for  $\kappa_1$  in Eq. (33).

**Table 1.** Combinations of  $\alpha$ ,  $\beta_1$  and  $\beta_2$  for which the dynamo period  $P_{\text{dyn}} = 22$  years and the mean-field decay time  $\tau_{\text{dec}} = 220$  years.

$\alpha$ [cm s <sup>-1</sup> ]	$\beta_1$ [cm <sup>2</sup> s <sup>-1</sup> ]	$\beta_2$ [cm <sup>2</sup> s <sup>-1</sup> ]	$f_\beta$	$C$
-25	$5.31 \times 10^{10}$	$6.12 \times 10^{11}$	$8.68 \times 10^{-2}$	-23.2
-50	$2.80 \times 10^{10}$	$9.24 \times 10^{11}$	$3.03 \times 10^{-2}$	-7.11
-150	$1.72 \times 10^{10}$	$1.55 \times 10^{12}$	$1.11 \times 10^{-2}$	-2.75
-500	$1.25 \times 10^{10}$	$2.61 \times 10^{12}$	$4.80 \times 10^{-3}$	-1.42

The poorly known value of  $\alpha$  is varied between  $-25$  and  $-500$  cm s<sup>-1</sup>. An upper limit on  $|\alpha|$  is given by  $l\Omega$ , where  $l$  is a typical convective length scale and  $\Omega \approx 2 \times 10^{-6}$  s<sup>-1</sup> is the solar rotation rate (Stix 1989, Ch. 8). Near the base of the convection zone we may estimate  $l \approx 10^9$  cm, so that  $l\Omega \approx 2 \times 10^3$  cm s<sup>-1</sup>. This is an upper limit, because the value of  $\alpha$  depends on the correlation between the turbulent velocity field  $\mathbf{u}_1$  and the vorticity  $\nabla \times \mathbf{u}_1$  (Sect. 4.3). The chaotic nature of the convection zone suggests that this correlation may be weak, i.e.  $|\alpha| \ll l\Omega$ .

The fundamental mode of  $\mathbf{B}_0$  should have  $P_{\text{dyn}} = 22$  years and  $\tau_{\text{dec}} \approx 10P_{\text{dyn}}$ , i.e.  $\omega = \omega_\odot = 9.05 \times 10^{-9}$  s<sup>-1</sup> and  $\gamma = \gamma_\odot = 1.44 \times 10^{-10}$  s<sup>-1</sup>. In order to meet these criteria we proceed as follows. Starting with a first guess of the required values of  $\beta_1$  and  $\beta_2$ , we solve the dispersion relation and find the eigenvalue  $\lambda$  of the fundamental mode. We repeat this by applying successive corrections to  $\beta_1$  and  $\beta_2$ , until  $\omega = \omega_\odot$  and  $\gamma = \gamma_\odot$ .

From Table 1 we see that for such solutions, a smaller value of  $|\alpha|$  requires a larger ratio  $f_\beta$ . This provides a lower limit to  $\alpha$ , since  $f_\beta$  should satisfy  $f_\beta \ll 1$ ; the smallest adopted value of  $|\alpha|$  is 25 cm s<sup>-1</sup>. Fig. 2 shows a typical solution.

## 4. The mean magnetic energy

### 4.1. Equations

The arguments presented in Sect. 2 lead to the following equation for  $\mathbf{T}$ , which is a modified version of that derived by Knobloch (1978) and Hoyng (1987):

$$\begin{aligned}
(\partial_t + \mathbf{u}_0 \cdot \nabla) T_{ij} &= \sum_{kl} \nabla_k (\alpha \epsilon_{ikl} T_{lj} + \alpha \epsilon_{jkl} T_{li}) \\
&+ \sum_k \{ (\nabla_k u_{0i}) T_{kj} + (\nabla_k u_{0j}) T_{ki} \} \\
&+ \frac{2}{5} \gamma (2 \sum_k T_{kk} \delta_{ij} - T_{ij}) + \nabla \cdot \beta \nabla T_{ij} - 2\nu T_{ij}. \quad (39)
\end{aligned}$$

The mean magnetic energy tensor is related to the mean magnetic stress tensor, which can be expressed in terms of  $\mathbf{T}$  as  $2T_{ij} - \epsilon \delta_{ij}$ , where  $\epsilon$  is the mean magnetic energy density,

$$\epsilon = \sum_i T_{ii}. \quad (40)$$

We employ the off-diagonal components of  $\mathbf{T}$  to define correlation coefficients of the field components:

$$C_{ij} \equiv \frac{T_{ij}}{\sqrt{T_{ii} T_{jj}}} = \frac{\langle B_i B_j \rangle}{\sqrt{\langle B_i^2 \rangle \langle B_j^2 \rangle}}. \quad (41)$$

These coefficients must satisfy  $|C_{ij}| \leq 1$ .

The advection term vanishes because the differential rotation  $\mathbf{u}_0$  (Eq. 4) is in the  $y$ -direction, and because only axisymmetric solutions are considered, i.e.  $\partial/\partial y = 0$ . For the gradient of  $\mathbf{u}_0$  in the overshoot layer we insert  $\nabla_i u_{0j} = a \delta_{ix} \delta_{jy}$ . Apart from  $\alpha$  and  $\beta$ , there is a third dynamo coefficient  $\gamma$ , related to the rms vorticity,

$$\gamma = \frac{1}{3} \tau_c \langle |\nabla \times \mathbf{u}_1|^2 \rangle. \quad (42)$$

It represents the creation of small-scale magnetic field due to the random field-line stretching by the convective motions. The effect of vorticity is to enhance the diagonal components of  $\mathbf{T}$  (i.e. the mean magnetic energy), but to decrease the off-diagonal components. The dissipative term  $-2\nu \mathbf{T}$  reduces all components of  $\mathbf{T}$  at the same rate and leaves the correlation coefficients unaffected.

As was argued in the introduction, we focus on the fundamental mode of Eq. (39), which should be non-periodic, marginally stable, axisymmetric ( $\partial/\partial y = 0$ ) and independent of latitude ( $\partial/\partial z = 0$ ).

Due to its symmetry,  $\mathbf{T}$  has only six independent tensor elements that can be conveniently arranged into one vector, whose components are  $T_\mu$ , with  $\mu = xx, xy, xz, yy, yz$  and  $zz$ . Applying Eq. (39) to the geometry of the Parker model, we obtain the following equations for  $T_\mu$  in the overshoot layer (region 1) and  $T'_\mu$  in the convection zone (region 2):

$$(\partial_t + 2\nu_1 - \beta_1 \partial_x^2) T_\mu = \sum_\nu (a X_{\mu\nu} + \frac{2}{5} \gamma_1 \Gamma_{\mu\nu}) T_\nu, \quad (43)$$

$$(\partial_t + 2\nu_2 - \beta_2 \partial_x^2) T'_\mu = \sum_\nu (\alpha \Xi_{\mu\nu} \partial_x + \frac{2}{5} \gamma_2 \Gamma_{\mu\nu}) T'_\nu. \quad (44)$$

Here  $\Gamma$ ,  $\mathbf{X}$  and  $\Xi$  are constant matrices, presented in Appendix B. From Eqs. (40) and (43–44), we obtain the equations governing the mean magnetic energy density in the two dynamo regions:

$$\partial_t \epsilon_1 = 2a T_{xy} + (2\gamma_1 - 2\nu_1 + \beta_1 \partial_x^2) \epsilon_1, \quad (45)$$

$$\partial_t \epsilon_2 = (2\gamma_2 - 2\nu_2 + \beta_2 \partial_x^2) \epsilon_2. \quad (46)$$

Vorticity and differential rotation are sources of mean magnetic energy. The former contributes equally to all diagonal components of  $\mathbf{T}$ , while the latter contributes to  $T_{yy}$ , the mean energy in the azimuthal field, but not to  $T_{xx}$  and  $T_{zz}$ . The source term for  $T_{yy}$  due to differential rotation is  $2a T_{xy}$ , and closer inspection of Eq. (43) shows that this term is generated from  $T_{xx}$ , the mean energy in the radial magnetic field. Thus the effect of differential rotation may be schematically represented as  $T_{xx} \rightarrow T_{xy} \rightarrow T_{yy}$ . On its turn,  $T_{xx}$  is produced entirely by vorticity. Hence, differential rotation enhances the magnetic energy

by converting radial field, generated by vorticity, into toroidal field. Turbulent diffusion enables transport of mean magnetic energy along the  $x$ -axis, and resistive dissipation converts the magnetic field into heat locally.

#### 4.2. Boundary conditions

For details of the boundary conditions, which number 24, the reader is referred to Appendix C; here it suffice to give a general idea of their derivation. We integrate Eq. (39) over a small distance  $\delta$  along the  $x$ -axis on either side of a boundary, and we let  $\delta \downarrow 0$ , which yields

$$\llbracket \beta \partial_x T_{ij} + \alpha \sum_l (\epsilon_{ixl} T_{lj} + \epsilon_{jxl} T_{li}) \rrbracket = 0, \quad (47)$$

where  $\llbracket \dots \rrbracket$  indicates the jump at the boundary. This condition is applied at  $x = -d_1$  and  $x = 0$ . The magnetic energy flux at a given point is defined as

$$F = -\beta \partial_x \epsilon. \quad (48)$$

By definition, a net flux in the positive  $x$ -direction is positive. Eq. (47) implies that  $F$  vanishes at  $x = -d_1$  and that it is continuous at  $x = 0$ . We also assume continuity of  $\mathbf{T}$  at  $x = 0$ . The boundary conditions at  $x = d_2$ , the convection zone - vacuum interface, are less trivial. We assume that here the energy flux is proportional to the energy density itself, i.e.

$$(\partial_x + \frac{\kappa_0}{d_2}) \epsilon_2 = 0 \quad \text{at } x = d_2. \quad (49)$$

Here  $\kappa_0$  is a dimensionless constant that measures approximately the ratio of the efficiency of energy transport through the surface at  $x = d_2$  and through the bulk of the convection zone. The nature of the energy transport at the convection zone - vacuum interface is discussed in detail in Van Geffen & Hoyng (1993). These authors estimate that  $\kappa_0$  is of the order 30 – 300.<sup>1</sup> The value of  $\kappa_0$  affects the decline of  $\mathbf{T}$  near  $x = d_2$ , but has a negligible effect on the solutions in the bulk of the dynamo, as is the case for all the boundary conditions at  $x = d_2$ . This is expected, since the dynamo is seated near the interface of the two regions, while the upper part of the convection zone plays only a passive role. The remaining conditions at  $x = d_2$  are presented in Appendix C.

#### 4.3. Constraints on the parameters

The normalised helicity  $H$  in the convection zone is defined as

$$H \equiv -\frac{\alpha}{\sqrt{\beta_2 \gamma_2}} = \frac{\langle \mathbf{u}_1 \cdot (\nabla \times \mathbf{u}_1) \rangle}{\sqrt{\langle |\mathbf{u}_1|^2 \rangle \langle |\nabla \times \mathbf{u}_1|^2 \rangle}}. \quad (50)$$

It measures the correlation between  $\mathbf{u}_1$  and the vorticity  $\nabla \times \mathbf{u}_1$ , and it obeys a Schwartz-type inequality:

$$|H| \leq 1. \quad (51)$$

<sup>1</sup> Van Geffen & Hoyng (1993) use  $(\partial_x + 1/\rho) \epsilon = 0$  at the upper surface of the convection zone and find  $R_{\odot}/\rho \approx 100 - 1000$ , where  $\rho = d_2/\kappa_0$ , so that  $\kappa_0 \approx 0.3R_{\odot}/\rho \approx 30 - 300$ .

For given  $\alpha$  and  $\beta_2$ , this implies a lower bound on  $\gamma_2$ . No reliable estimate for  $H$  is known, but it is likely that  $|H| \ll 1$  (Moffatt 1978, Ch. 11). In the overshoot region condition (51) is automatically satisfied because  $\alpha$  is neglected there.

A second constraint is based on the following estimate of the typical length scale of the turbulence in the convection zone (Eqs. 2 and 42):

$$l_t \equiv \sqrt{\frac{\beta_2}{\gamma_2}} \leq d_2. \quad (52)$$

Obviously the turbulent length scale, i.e. the typical size of a convective cell, should not exceed the thickness of the convection zone. Hence there is the condition  $l_t \leq d_2$ , which implies another lower bound on  $\gamma_2$ .

The central idea of Parker (1993) is that strong magnetic fields suppress the turbulence in the overshoot layer. For simplicity we assume that  $\gamma$  is suppressed by the same factor  $f_\beta \ll 1$  as  $\beta$ :

$$\frac{\gamma_1}{\gamma_2} = f_\beta. \quad (53)$$

#### 4.4. Solution of Eqs. (43–44)

We separate the time dependence of  $\mathbf{T}$  using the following ansatz:

$$T_\mu(x, t) = \tilde{T}_\mu(x) e^{\Lambda t}, \quad (54)$$

and similarly for  $T'_\mu$ . The general solution of Eqs. (43–44) is presented in Appendix B. The boundary conditions constitute 24 relations between the integration constants, whose determinant should vanish. Every root  $\Lambda$  of this dispersion relation corresponds to a separate mode. We are only interested in the mode with the largest growth rate  $\text{Re } \Lambda$  (the fundamental mode). As we argued in the Introduction, this mode should be non-periodic ( $\text{Im } \Lambda = 0$ ). It has been observed before, that this is indeed always the case (Van Geffen & Hoyng 1993), although no formal proof is available. By themselves, the oscillating modes are unphysical because they have a magnetic energy of alternating sign. They play a role as transients in initial value problems, which we are not considering here.

### 5. Case A: no resistive dissipation ( $\nu_1 = \nu_2 = 0$ )

In this section we focus on verifying whether solutions with  $\nu_1 = \nu_2 = 0$  are physically acceptable, postponing a more detailed discussion of the various tensor elements of  $\mathbf{T}$  to Sect. 6.

#### 5.1. Parameters

We set  $l_t = d_2$  and thereby adopt the minimal value of  $\gamma_2$  that is compatible with Eq. (52). As it turns out, Eq. (51) is then satisfied by a large margin, for all the marginally stable solutions of case A (Table 2). We adopt four different ratios  $f_\beta$ , namely  $10^{-1}$ ,  $10^{-2}$ ,  $10^{-3}$  and  $10^{-4}$ . Then  $\gamma_1$  follows from Eq. (53). The

**Table 2.** Parameters that result in marginal stability of T, with  $\nu_1 = \nu_2 = 0$  and  $l_t/d_2 = 1$ .

run	$\kappa_0$	$f_\beta$	$\beta_2$ [cm <sup>2</sup> s <sup>-1</sup> ]	$\gamma_2$ [s <sup>-1</sup> ]	$H$
A1	100	10 <sup>-1</sup>	3.1 × 10 <sup>14</sup>	7.8 × 10 <sup>-7</sup>	9.6 × 10 <sup>-3</sup>
A2	''	10 <sup>-2</sup>	5.5 × 10 <sup>14</sup>	1.4 × 10 <sup>-6</sup>	5.4 × 10 <sup>-3</sup>
A3	''	10 <sup>-3</sup>	1.6 × 10 <sup>15</sup>	4.1 × 10 <sup>-6</sup>	1.8 × 10 <sup>-3</sup>
A4	''	10 <sup>-4</sup>	7.1 × 10 <sup>15</sup>	1.8 × 10 <sup>-5</sup>	4.2 × 10 <sup>-4</sup>
A5	300	10 <sup>-1</sup>	3.0 × 10 <sup>14</sup>	7.4 × 10 <sup>-7</sup>	1.0 × 10 <sup>-2</sup>
A6	''	10 <sup>-2</sup>	5.3 × 10 <sup>14</sup>	1.3 × 10 <sup>-6</sup>	5.7 × 10 <sup>-3</sup>
A7	''	10 <sup>-3</sup>	1.6 × 10 <sup>15</sup>	4.0 × 10 <sup>-6</sup>	1.9 × 10 <sup>-3</sup>
A8	''	10 <sup>-4</sup>	7.0 × 10 <sup>15</sup>	1.8 × 10 <sup>-5</sup>	4.3 × 10 <sup>-4</sup>

$\alpha$ -coefficient plays an insignificant role in the energy equation, and a change in its value has a negligible effect on the growth rate  $\Lambda$ . For this reason we do not vary  $\alpha$  in Eq. (44), but set  $\alpha = -150$  cm s<sup>-1</sup>. We adopt two values for  $\kappa_0$ , namely 100 and 300. The parameters  $d_1$ ,  $d_2$  and  $a$  are as indicated in Fig. 1.

We obtain marginally stable solutions in the following way. After making an initial guess of the required value of  $\beta_2$ , we solve the dispersion relation and obtain the growth rate  $\Lambda$  of the fundamental mode. We then apply successive corrections to  $\beta_2$ , while keeping  $f_\beta$  and  $l_t$  constant, until  $\Lambda$  equals zero. The physical idea behind this method is that we vary the efficiency of turbulent transport to the solar surface, the only energy sink in the dynamo in case A, until the marginally stable state is reached. The required values of  $\beta_2$  and the corresponding values of  $\gamma_2$  and  $H$  are shown in Table 2. Since  $l_t/d_2$  may in fact be smaller than unity, we may underestimate  $\gamma_2$  and hence also the energy production rate due to vorticity. Therefore the values of  $\beta_2$  must be understood as *minimal* values, required for marginal stability. Marginal stability of T is reached only if  $\beta_2 \gtrsim 3 \times 10^{14}$  cm<sup>2</sup> s<sup>-1</sup>, a very high value also found by Van Geffen (1993a).

### 5.2. Implications for the mean magnetic field

The diffusivities that are required for marginal stability of T are at least a factor 10<sup>2</sup> larger than the values that were adopted for the mean-field equation (Table 1). The effect of such large diffusivities on the mean field can be clarified with the help of Eq. (35), which provides an estimate of the dynamo frequency  $\omega$ . If  $\omega = \omega_\odot$  and  $\beta_2 = 3 \times 10^{14}$  cm<sup>2</sup> s<sup>-1</sup>, say, then  $\omega/\beta_2 k_z^2 \approx 3 \times 10^{-3} \ll 1$ , so that  $|C| \ll 1$ . Then Eq. (35) reduces to

$$\omega \approx \beta_2 k_z^2 |C|/4 = \frac{\beta_1 a |\alpha|}{4 \beta_2^2 k_z}, \quad (55)$$

which, after substitution of  $\omega_\odot$ ,  $a$  and  $k_z$ , yields the following estimate of the value of  $|\alpha|$ , required for the mean field to have a 22-year period:

$$|\alpha| \approx 9 \times 10^{-13} \beta_2 / f_\beta. \quad (56)$$

Although  $\alpha$  does formally appear in Eq. (43–44), it has a negligible influence on the growth rate  $\Lambda$ . In other words, T remains close to marginal stability, even if a different value of  $\alpha$

is adopted. Hence we have some liberty to change  $\alpha$  for a given solution of Eqs. (43–44). The values of  $\beta_2$  presented in Table 2 imply that  $|\alpha|$  must be of the order  $3 \times 10^3 - 6 \times 10^5$  cm s<sup>-1</sup> (Eq. 56). But we have the following two upper limits for  $|\alpha|$ . First, there is condition (51). Since the solutions presented in Table 2 all have  $l_t/d_2 = 1$ , we may employ Eq. (52) to write this condition in the form  $|\alpha| \leq \beta_2/d_2$ . Second,  $|\alpha|$  should not exceed the typical maximum value  $l\Omega \approx 2 \times 10^3$  cm s<sup>-1</sup> in the lower part of the convection zone (Sect. 3.4). Commonly  $|\alpha|$  is believed to be about a factor 10<sup>2</sup> smaller. Some of the required values of  $\alpha$  violate condition (51), and all of them exceed  $l\Omega$ . In other words,  $\alpha$  would have to be unphysically large to counteract the strong turbulent diffusion and produce a dynamo period of 22 years.

### 5.3. Root mean square magnetic field strength

Since T is solved from a linear equation with linear boundary conditions, it is determined up to an arbitrary multiplicative factor. We calibrate T by using reference values, based on observations, for the magnetic energy flux,  $F = -\beta \partial_x \epsilon$ , and for the rms field strength,

$$B_{\text{rms}} = \sqrt{8\pi\epsilon}. \quad (57)$$

Three estimates are considered here, and our aim is to verify whether marginally stable solutions with  $\nu_1 = \nu_2 = 0$  can reproduce all three simultaneously.

- 1) Active regions and small flux tubes, which are known to have a field strength of about 10<sup>3</sup> G, cover about 1% of the solar surface during the solar maximum, so that  $B_{\text{rms}}(d_2) \approx \sqrt{10^{-2} \times 10^6} = 100$  G.
- 2) The rms field strength in the overshoot layer is believed to be about  $2 \times 10^4 - 10^5$  G.
- 3) The total energy flux, required for coronal heating, is estimated to be  $F_c \approx 5 \times 10^6$  erg cm<sup>-2</sup> s<sup>-1</sup> (Withbroe & Noyes 1977, Kuperus et al. 1981). This flux may be provided by the magnetic energy flux through the upper surface of the convection zone, which after inserting Eqs. (49) and (57) can be expressed as

$$F_s \equiv F(x = d_2) = \frac{\beta_2 \kappa_0 B_{\text{rms}}^2(x = d_2)}{8\pi d_2}. \quad (58)$$

Presumably this energy flux is in the form of Alfvén waves.

Let us apply the first estimate and fix  $B_{\text{rms}}(d_2) = 100$  G. The resulting values of  $F_s$ , shown in Table 3, are at least two orders of magnitude larger than  $F_c$ . These numbers can be reduced only by adopting much *smaller* values for  $\beta_2$  or  $\kappa_0$ , such that  $\beta_2 \kappa_0$  is reduced by at least a factor of the order 100. But  $\beta_2$  is determined by the constraint of marginal stability and we cannot decrease  $\kappa_0$  as much as would be required.

From estimates 1) and 2) it follows that the ratio of maximum rms field strength to rms surface field strength,

$$r_B \equiv \frac{\max B_{\text{rms}}(x)}{B_{\text{rms}}(d_2)}, \quad (59)$$



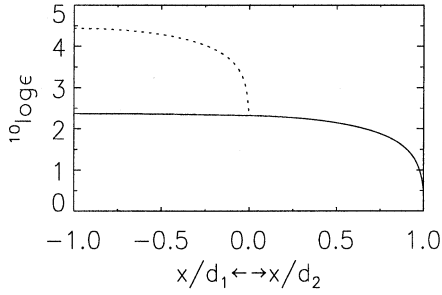


**Fig. 3.** Mean magnetic energy density  $\epsilon$  as a function of  $x$  ( $\epsilon$  is set to 1 at  $x = d_2$ ) for two marginally stable solutions with  $\nu_1 = \nu_2 = 0$  (drawn curve: A1; dashed curve: A4). For case A1 ( $f_\beta = 0.1$ ), the transition from the overshoot layer to the convection zone is quite smooth (in this plot the discontinuity in  $\partial_x \epsilon$  is coincidentally removed due to the stretching of the  $x$ -coordinate in the overshoot layer). For case A4 ( $f_\beta = 10^{-4}$ ) the transition is sharp: the smaller  $f_\beta$ , the less efficient turbulent transport is in the overshoot layer, and the higher the resulting concentration of magnetic energy.

**Table 3.** Values of  $r_B$  and  $F_s$  for marginally stable solutions with  $\nu_1 = \nu_2 = 0$ ,  $\alpha = -150 \text{ cm s}^{-1}$  and  $l_i/d_2 = 1$ . The values of  $F_s$  are calibrated by assuming  $B_{\text{rms}}(d_2) = 100 \text{ G}$ .

run	$r_B$	$F_s$ [erg cm $^{-2}$ s $^{-1}$ ]
A1	8.8	$6.2 \times 10^8$
A2	12	$1.1 \times 10^9$
A3	32	$3.2 \times 10^9$
A4	95	$1.4 \times 10^{10}$
A5	15	$1.8 \times 10^9$
A6	22	$3.2 \times 10^9$
A7	55	$9.5 \times 10^9$
A8	170	$4.1 \times 10^{10}$

should be of the order  $200 \lesssim r_B \lesssim 1000$ . In Table 3 we present the values of  $r_B$  for marginally stable solutions with  $\nu_1 = \nu_2 = 0$ . None of these are within the required range. The value of  $r_B$  depends on  $f_\beta$  and  $\kappa_0$ . The smaller  $f_\beta$ , i.e. the less efficient turbulent diffusion in the overshoot layer is, the more magnetic energy accumulates there, and the larger  $r_B$  becomes. This effect is demonstrated in Fig. 3. We could achieve better agreement for  $r_B$  by adopting some value  $f_\beta < 10^{-4}$ , but we have not pursued this, since the constraint of marginal stability would require a turbulent diffusivity  $\beta_2$  larger than  $7 \times 10^{15} \text{ cm}^2 \text{ s}^{-1}$  (see Table 2). This would cause a further increase of  $F_s$ . The effect of a change in  $\kappa_0$  can be inferred from Eq. (46) and boundary condition (49), which yield the following marginally stable solution:

$$\frac{\epsilon_2(x)}{\epsilon_2(d_2)} = \frac{1}{2} \left( \frac{\kappa_0}{k_7 d_2} + 1 \right) e^{-k_7(x-d_2)} - \frac{1}{2} \left( \frac{\kappa_0}{k_7 d_2} - 1 \right) e^{k_7(x-d_2)} \quad (0 \leq x \leq d_2), \quad (60)$$

where  $k_7 = \sqrt{(\Lambda + 2\nu_2 - 2\gamma_2)/\beta_2}$ . Hence we can increase  $r_B$  by increasing  $\kappa_0$ , as is demonstrated in Table 3 (compare e.g.

**Table 4.** Case B: vorticity coefficients, turbulent length scales, dissipation coefficients and corresponding dissipative timescales (in months) for marginally stable solutions, with  $\beta_1$  and  $\beta_2$  as in Table 1, and  $30 \lesssim \kappa_0 \lesssim 300$ .

run	$H$	$\alpha$ [cm s $^{-1}$ ]	$\gamma_2$ [*]	$l_i/d_2$	$\nu$ [*]	$1/2\nu$ [mo]
B1	1.00	-50	0.0027	0.92	0.061	3.12
B2	"	-150	0.014	0.52	0.082	2.33
B3	"	-500	0.096	0.26	0.14	1.33
B4	0.71	-25	0.0020	0.87	0.074	2.56
B5	"	-50	0.0054	0.65	0.078	2.45
B6	"	-150	0.029	0.37	0.10	1.83
B7	"	-500	0.19	0.18	0.22	0.89
B8	0.32	-25	0.010	0.39	0.13	1.44
B9	"	-50	0.027	0.29	0.14	1.41
B10	"	-150	0.15	0.16	0.20	0.96
B11	"	-500	0.96	0.08	0.95	0.20
B12	0.10	-25	0.10	0.12	0.30	0.64
B13	"	-50	0.27	0.09	0.32	0.60
B14	"	-150	1.4	0.05	1.4	0.13
B15	0.05	-25	0.41	0.06	0.49	0.39
B16	"	-50	1.1	0.05	1.1	0.18

\* in units of  $10^{-6} \text{ s}^{-1}$

runs A1 and A5). Unfortunately, this would also result in a larger  $F_s$  (Eq. 58).

#### 5.4. Summary

We may summarise the findings of Sect. 5 as follows. If resistive dissipation is neglected, then the resulting solutions T are unlikely to describe the solar dynamo, for three reasons, the first two of which are a direct consequence of the abnormally high turbulent diffusivities ( $\beta_2 \gtrsim 3 \times 10^{14} \text{ cm}^2 \text{ s}^{-1}$ ), required for marginal stability of T:

- ⊙ a value of  $\beta_2 \gtrsim 3 \times 10^{14} \text{ cm}^2 \text{ s}^{-1}$  is incompatible with a dynamo period of 22 years;
- ⊙ the magnetic energy flux through, and the rms field strength at the upper boundary of the convection zone cannot *both* assume solar values;
- ⊙  $r_B$ , the ratio of maximum rms field strength to rms surface field strength, is too small.

#### 6. Case B: uniform resistive dissipation ( $\nu_1 = \nu_2 \neq 0$ )

In the previous section we did not succeed in obtaining a consistent dynamo model on the basis of the finite energy method. Apparently we require an extra energy sink, possibly due to resistive dissipation. For this reason we now turn to the case  $\nu_1, \nu_2 \neq 0$ , and we make the simplest possible approximation:

$$\nu_1 = \nu_2 = \nu. \quad (61)$$

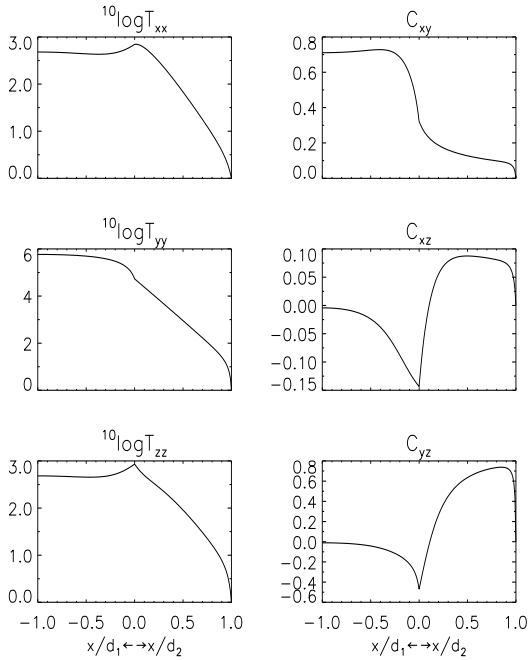


**Fig. 4.** Diagonal components of the mean magnetic energy tensor  $\mathbf{T}$  and correlation coefficients  $C_{ij}$  as a function of  $x$  ( $T_{yy}$  is set to 1 at  $x = d_2$ ), for a marginally stable solution with little vorticity (B5). Note the large, predominantly toroidal field ( $B_y$ ) in the overshoot layer and its strong correlation with the radial field ( $B_x$ ). In the convection zone, there is a strong correlation between  $B_z$  and  $B_y$ .

Under this assumption, our treatment of resistive dissipation amounts to the introduction of a global decay factor  $e^{-2\nu t}$  for a given solution of Eqs. (43–44) *without* resistive dissipation.

### 6.1. Parameters

For the parameters  $\alpha$ ,  $\beta_1$  and  $\beta_2$  we employ the values shown in Table 1. For each of these combinations we fix  $\gamma_2$  by adopting several values of  $H$  in the range from  $H = 1$  to  $H = 0.05$ , under the condition that Eq. (52) is satisfied. Then  $\gamma_1$  follows from Eq. (53). Notice that Eqs. (51) and (52) now pose almost equally strong constraints on the parameters, as is demonstrated by the fact that  $l_t/d_2$  and  $H$ , which should both be smaller than unity, have the same order of magnitude (Table 4).

Here  $H = 1$  corresponds to maximal helicity, or minimal vorticity (Eq. 50). It is likely that  $|H| \ll 1$  (Sect. 4.3), but by decreasing  $|H|$  for fixed values of  $\alpha$  and  $\beta_2$ , the role of vorticity increases. Beyond a certain point, the energy production is dominated by random stretching of field lines, with only a negligible contribution of differential rotation. Such solutions are unlikely to describe the solar dynamo, since they do not exhibit strong, predominantly toroidal fields in the overshoot layer. Hence, for a given combination of  $\alpha$  and  $\beta_2$ , there is a lower limit on  $|H|$ . From numerical experience we conclude that for solutions with  $|H| \lesssim 0.05$ , the dominant source of magnetic energy is random field-line stretching.

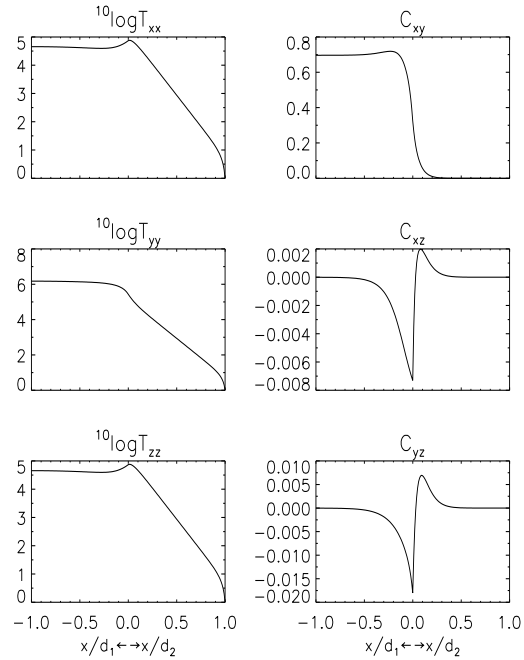


**Fig. 5.** Diagonal components of the mean magnetic energy tensor  $\mathbf{T}$  and correlation coefficients  $C_{ij}$  as a function of  $x$  ( $T_{yy}$  is set to 1 at  $x = d_2$ ), for a marginally stable solution with strong vorticity (B15). Compared to Fig. 4, the toroidal magnetic field is less predominant and all  $C_{ij}$  are reduced, except  $C_{xy}$  in the overshoot layer.

In most cases, we adopt  $\kappa_0 = 100$ , but in some cases we use a different value. The reason for this is explained in Sect. 6.3. However, it turns out that the values of  $\nu$ , required for marginal stability of  $\mathbf{T}$  are, within the given accuracy of Table 4, insensitive to these changes of  $\kappa_0$ .

### 6.2. Solutions

Two examples of marginally stable solutions are shown in Figs. 4 and 5. As will be argued in Sect. 6.3, these solutions appear to be reasonable models of the solar dynamo. The main features of Fig. 4 are as follows:

- ⊙ the diagonal components of  $\mathbf{T}$  reach a maximum in the overshoot layer, and decline almost exponentially throughout the convection zone, until the onset of a more rapid decline near the upper surface;
- ⊙ the dominant component of  $\mathbf{T}$  is  $T_{yy}$ , the mean magnetic energy in the toroidal field. This is a consequence of differential rotation;
- ⊙ as a result of differential rotation, which creates toroidal field ( $B_y$ ) from radial field ( $B_x$ ), there is a strong correlation between  $B_x$  and  $B_y$  in the overshoot layer;
- ⊙ there is a strong correlation between  $B_y$  and  $B_z$  in the convection zone due to the  $\alpha$ -effect;
- ⊙ if we integrate Eqs. (45–46) over  $x$ , we obtain the energy balance, given by

$$\partial_t E = Q_{\text{tot}} - Q_{\text{diss}} - F_s = 0. \quad (62)$$

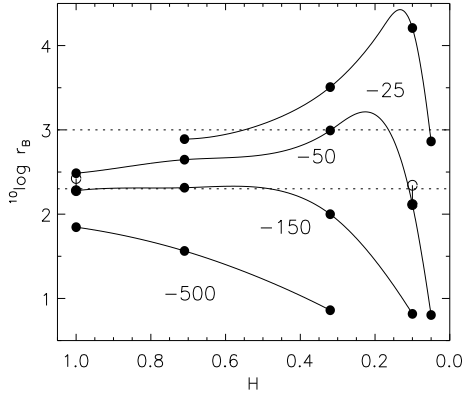


**Fig. 6.** Ratio  $r_B$  of maximal rms field strength to rms surface field strength for various models of case B, plotted versus the normalised helicity  $H$ . The full circles denote solutions with  $\kappa_0 = 100$ . The drawn curves are interpolations between solutions with identical values of  $\alpha$ , from  $\alpha = -25 \text{ cm s}^{-1}$  (top curve) to  $\alpha = -500 \text{ cm s}^{-1}$  (bottom curve). The area between the dotted lines indicates the estimated range of  $r_B$  for the Sun. In two cases we have adjusted  $r_B$  by changing  $\kappa_0$  (open circles).

Here  $E$  is the total magnetic energy per unit of surface area, given by  $E = E_1 + E_2$ , where  $E_1 = \int_{-d_1}^0 dx \epsilon_1$  and  $E_2 = \int_0^{d_2} dx \epsilon_2$ ;  $Q_{\text{tot}}$  is the total energy production rate, i.e.

$$Q_{\text{tot}} = 2a \int_{-d_1}^0 dx T_{xy} + 2\gamma_1 E_1 + 2\gamma_2 E_2, \quad (63)$$

and  $Q_{\text{diss}}$  is the total rate of resistive dissipation, given by

$$Q_{\text{diss}} = 2\nu_1 E_1 + 2\nu_2 E_2. \quad (64)$$

Table 5 shows that  $F_s$  accounts for less than  $10^{-3}$  times  $Q_{\text{tot}}$ , i.e. the dominant energy sink turns out to be resistive dissipation. This is due to the low efficiency of turbulent transport.

The solution presented in Fig. 5 has a smaller normalized helicity  $H$ . We recall that this is equivalent to a larger vorticity  $\gamma_2$  (for given  $\alpha$  and  $\beta_2$ ). The main differences between Figs. 4 and 5 are as follows:

- ⊙ the dominance of  $T_{yy}$  is reduced, because vorticity enhances  $T_{xx}$ ,  $T_{yy}$  and  $T_{zz}$  at the same rate;
- ⊙ most correlation coefficients are reduced, due to the increase in vorticity. However,  $C_{xy}$  is not reduced in the overshoot layer, because here  $T_{yy}$  is mainly created by differential rotation from  $T_{xx}$  and not *directly* by vorticity. This results in a strong correlation between  $B_x$  and  $B_y$ , almost irrespective of the value of  $\gamma_1$  and  $\gamma_2$  (see Sect. 4.1).

### 6.3. Root mean square magnetic field strength

Fig. 6 shows  $r_B$  as a function of  $H$  for models B1, B2,  $\dots$ , B16 (Table 4). For a subset of solutions, indicated in Table 5,  $r_B$  agrees with solar estimates, i.e.  $200 \lesssim r_B \lesssim 1000$ . This good agreement is possible because if  $\nu$  is sufficiently large, the convection zone becomes a net sink of energy, resulting

**Table 5.** Values of  $\kappa_0$  and  $F_s$  for marginally stable solutions that are reasonable as models for the solar dynamo. The values of  $F_s$  are calibrated by assuming  $B_{\text{rms}}(d_2) = 100 \text{ G}$ .

run	$\kappa_0$	$F_s$ [erg cm $^{-2}$ s $^{-1}$ ]	$F_s/Q_{\text{tot}}$
B1	100	$1.8 \times 10^6$	$2.3 \times 10^{-4}$
B2	200	$6.2 \times 10^6$	$6.6 \times 10^{-4}$
B4	100	$1.2 \times 10^6$	$1.9 \times 10^{-5}$
B5	100	$1.8 \times 10^6$	$8.8 \times 10^{-5}$
B6	100	$3.1 \times 10^6$	$4.3 \times 10^{-4}$
B9	100	$1.8 \times 10^6$	$1.0 \times 10^{-5}$
B13	300	$5.5 \times 10^6$	$2.0 \times 10^{-4}$
B15	100	$1.2 \times 10^6$	$2.7 \times 10^{-6}$

in an exponential decay of  $\epsilon$  throughout most of the convection zone. Without resistive dissipation this effect cannot occur for marginally stable solutions, since  $k_7$  is then purely imaginary (Eq. 60). On most occasions we adopted  $\kappa_0 = 100$ , but in two cases we used a different value in order to improve agreement for  $r_B$ . These modified solutions are indicated by the open symbols in Fig. 6. With the present calibration, the magnetic energy flux through the solar surface for solutions with  $200 \lesssim r_B \lesssim 1000$  is of the order  $F_s \approx (1 - 6) \times 10^6 \text{ erg cm}^{-2} \text{ s}^{-1}$  (Table 5), i.e. comparable to the flux required for coronal heating,  $F_c \approx 5 \times 10^6 \text{ erg cm}^{-2} \text{ s}^{-1}$ . This agreement results from the much smaller turbulent diffusivities employed here ( $\beta_2 \approx 10^{12} \text{ cm}^2 \text{ s}^{-1}$ ), compared to those required in Sect. 5 ( $\beta_2 \gtrsim 3 \times 10^{14} \text{ cm}^2 \text{ s}^{-1}$ ).

Hence, by including resistive dissipation, and setting  $\nu_1 = \nu_2$ , we are able to obtain solutions for T that reproduce approximately the correct values of both  $r_B$  and  $F_s$ . For these solutions, the timescale for resistive dissipation is  $1/2\nu \approx 1$  month, comparable to the convective turnover time. We discuss this issue further in Sect. 8.

### 7. Case C: reduced dissipation in the overshoot layer ( $\nu_1 \ll \nu_2$ )

If a strong, large-scale azimuthal magnetic field exists in the overshoot layer, then small-scale structures are less likely to form there than in the convection zone. Hence it is perhaps more realistic to assume that in the overshoot layer resistive dissipation is less efficient than in the convection zone, i.e.  $\nu_1 \ll \nu_2$ .<sup>2</sup> In this section, we briefly examine that possibility, assuming that  $\nu_1/\nu_2$  is reduced to the same value as  $\beta_1/\beta_2$  and  $\gamma_1/\gamma_2$ , i.e.

$$\frac{\nu_1}{\nu_2} = f\beta. \quad (65)$$

Our aim is to explore the effect of this assumption on a typical solution with  $\nu_1 = \nu_2 \neq 0$ , obtained previously in Sect. 6 (case B). To that purpose we vary  $\nu_1$  iteratively, while keeping  $\nu_1/\nu_2$  fixed, until the marginally stable state is reached. Fig. 7 shows the distribution of mean magnetic energy for such a solution.

<sup>2</sup> We thank dr. M. Schüssler for this suggestion

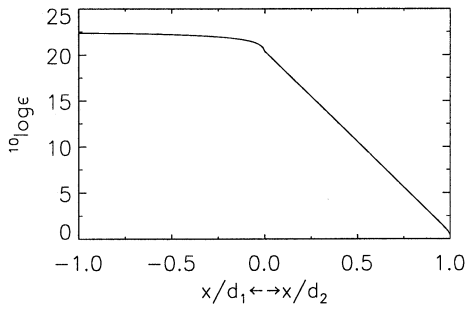


**Fig. 7.** Mean magnetic energy density  $\epsilon$  as a function of  $x$  ( $\epsilon$  is set to 1 at  $x = d_2$ ) for a marginally stable solution with  $\nu_1 = 7.2 \times 10^{-8} \text{ s}^{-1}$  and  $\nu_2 = 2.4 \times 10^{-6} \text{ s}^{-1}$  (case C with  $\nu_1/\nu_2 = f_\beta$ ). The remaining parameters are as in case B5.

The main differences with case B5, relevant for our discussion, are as follows:

- ⊙ the required value of  $\nu_2$  is much larger (by a factor of about 30);
- ⊙ the required value of  $\nu_1$  is only slightly smaller;
- ⊙ there is a much more rapid decline of  $\epsilon$  throughout the convection zone (about 20 decades;  $r_B = 8.8 \times 10^{10}$ ).

The first two points indicate that a small reduction in  $\nu_1$ , compared to its value in case B, has to be compensated by a large increase in  $\nu_2$ . This effect can be explained as follows. If we decrease resistive dissipation in the overshoot layer, than transport of magnetic energy out of the overshoot layer should increase, in order to achieve marginal stability of  $T$ . Therefore the gradient of the magnetic energy density in the overshoot layer,  $\partial_x \epsilon_1$ , has to steepen. Since there is continuity of energy flux, this can be achieved by sharpening the gradient in the convection zone, i.e. by increasing resistive dissipation there ( $\nu_2$ ). However, this mechanism is rather indirect and inefficient, requiring a large increase in  $\nu_2$ .

The third point is a consequence of the strong resistive dissipation in the convection zone (large  $\nu_2$ ), leading to a steep gradient in the magnetic energy density (see Eq. 60). It follows that this model does not correspond to the solar dynamo, since  $r_B$  is many orders of magnitude larger than the highest estimated value (about  $10^3$ ) for the Sun.

It may be felt that  $\nu_1$  is still unrealistically large - indeed one's first intuition would to take  $\nu_1 = 0$ . However, this is not possible, because then even larger values of  $\nu_2$  would be required, leading to a further increase of  $r_B$ .

We may therefore summarize the results of this section as follows. If we want to balance the energy production in the overshoot layer without invoking resistive dissipation as a dominant energy sink in this region, then turbulent transport has to be made more efficient. This requires a steeper gradient of the magnetic energy density, which can be achieved by increasing resistive dissipation in the convection zone ( $\nu_2$ ). Compared to case B, there are two main effects. First, the dissipation time scale in the convection zone ( $1/2\nu_2$ ) becomes much shorter than the convective turnover time (about 1 month). This is problematic,

as will be argued in the Discussion. Second, the ratio  $r_B$  is very large, and for this reason case C does not appear to correspond to the solar dynamo.

## 8. Summary and discussion

We have studied the Parker's 'surface-wave dynamo' (Parker 1993) by solving equations for the mean magnetic field  $B_0$  and for the mean magnetic energy tensor  $T$ . The mean quantities are interpreted as ensemble averages, so that the dynamo parameters may be treated as constants. In solving the mean-field equation, we chose the parameters in such a way, that  $B_0$  has a period of 22 years and a decay time of about 10 dynamo periods. This slight sub-criticality of  $B_0$  is motivated by the concept of phase mixing, which arises in the ensemble average due to variability in the dynamo period.

The equation for  $T$  was solved under the constraint of marginal stability. If resistive dissipation is ignored, this requires a turbulent diffusivity of the order  $\beta_2 \gtrsim 3 \times 10^{14} \text{ cm}^2 \text{ s}^{-1}$ . Consequently,  $\alpha$  has to be unphysically large for  $B_0$  to have a period of 22 years. Furthermore, the three calibrations of  $T$  that we employ, namely for the rms field strengths in the overshoot layer and at the solar surface, and for the magnetic energy flux through the solar surface, are inconsistent if  $\nu_1 = \nu_2 = 0$ .

Concerning the large turbulent diffusivities that are required if  $\nu_1 = \nu_2 = 0$ , we confirm the results of Van Geffen (1993b), who found similar values, in spite of the fact that the overshoot layer was badly resolved in his finite-grid calculation. It is evident that transport of mean magnetic energy by turbulent diffusion cannot provide an energy sink that is efficient enough to render  $T$  marginally stable. One conclusion of this paper is therefore that an additional energy sink, previously not accounted for, must be invoked to balance the energy budget.

A possible candidate investigated in this paper is resistive dissipation, which operates through an energy cascade from the largest scale down to the dissipative scale, where the magnetic energy is converted into heat. With respect to resistive dissipation, we pointed out a fundamental difference between  $B_0$  and  $T$ . Since  $B_0$  corresponds to the largest length scale of the dynamo, it is not affected by resistive dissipation, which operates at the smallest length scale. On the other hand,  $T$  has contributions from all length scales. Consequently, the scale dependence of resistive dissipation results in a closure problem. Our approach has been to apply the simplest possible, scale-independent approximation, and describe the average effect of resistive dissipation on  $T$  through a coefficient  $\nu$ .

With this heuristic treatment of resistive dissipation, we are able to comply with the conditions on  $B_0$  and  $T$ , posed by the finite-energy method. Admittedly, the finite-energy method loses some of its previous appeal, because we have no estimates or constraints for  $\nu$ , and simply adjust its value as to attain marginal stability of  $T$ . But by doing so, and setting  $\nu_1 = \nu_2$ , we are able to obtain solutions that correctly reproduce the three calibrations for  $T$ . Thus the inconsistencies, that arise when turbulent transport and subsequent loss at the surface are assumed

to provide the only sink of magnetic energy in the dynamo, are removed.

In these models, most of the energy loss in the dynamo results from resistive dissipation, and only a small fraction from turbulent transport to the boundary. We find that the timescale for resistive dissipation needs to be of the order of one month. This is comparable to the eddy turnover time, the characteristic timescale for the energy cascade. In numerical simulations of hydromagnetic convection by Nordlund et al. (1992), a similar timescale for ohmic decay was found. Due to the impenetrable boundaries that were employed by these authors, the importance of energy transport out of the dynamo region cannot be assessed from their calculations. Relevant for our discussion is their result that the magnetic energy of a small-scale dynamo in the convection zone can attain a stationary state through a balance with resistive dissipation, and that the entire magnetic energy is converted within one convective turnover time. Whether their result also applies to the overshoot layer is uncertain. Here the magnetic field is believed to be strong and well-ordered, so that turbulence is suppressed, and small-scale structures, essential for resistive dissipation, are less likely to develop. Hence, although our results are consistent with those of Nordlund et al. (1992), we probably overestimate the dissipation rate in the overshoot layer ( $\nu_1$ ). Given our simplified, linear treatment of the energy cascade, this is perhaps not too surprising.

Setting to zero or reducing resistive dissipation in the overshoot layer is not a fruitful option in the present model, because this makes it impossible to obtain a marginally stable solution that is also physically reasonable. It seems that turbulent diffusion is too inefficient in transporting a significant fraction of the produced magnetic energy out of the overshoot layer, unless  $\beta_1$  is very large, or the gradient of the magnetic energy density is very steep. The latter requires that the dissipation timescale in the convection zone ( $1/2\nu_2$ ) be much shorter than the convective turnover time, which is unlikely. We may speculate that the inefficiency of turbulent diffusion can be resolved by treating turbulent diffusivity not as a scalar but as a tensor, and enhancing the radial component relative to the other components in order to model schematically the effect of magnetic buoyancy. It is nevertheless consistent with the dynamo mechanism described by Eqs. (45–46) to allow some resistive dissipation in the overshoot layer, for the following reason. The production of magnetic energy results mainly from differential rotation, which amplifies the magnetic field created by vorticity. The  $\alpha$ -effect, responsible for the large-scale field, has little impact on the magnetic energy. In other words, the magnetic energy as described by Eqs. (45–46) mainly resides in small scales, so that resistive dissipation may be important in the convection zone as well as in the overshoot layer.

If we accept for the moment the dissipation rates of Sect. 6, we may estimate the total heat produced by resistive dissipation as  $AQ_{\text{diss}} = 2\nu AE$ , where  $A \approx 2 \times 10^{22} \text{ cm}^2$  is the area of a strip extending  $35^\circ$  on both sides of the equator, positioned at the base of the convection zone, and  $Q_{\text{diss}}$  is given by Eq. (64). Employing the calibration  $B_{\text{rms}}(d_2) = 100 \text{ G}$ , we obtain typical values of  $AE$  of the order  $10^{39} - 10^{40} \text{ erg}$ . The corresponding values of

$AQ_{\text{diss}}$  range from about  $0.04L_\odot$  up to values larger than  $L_\odot$ . Although we are clearly overestimating the value of  $AQ_{\text{diss}}$  in some cases, there are other indications that hint at the important role of resistive heating in the solar dynamo. It has been estimated that viscous and resistive heating in the convection zone can indeed amount to several percents of the convective flux, i.e. of the solar luminosity (Hewitt et al. 1975, Brandenburg 1993). A high dissipation rate poses in turn a strong demand on differential rotation, the main energy source of the dynamo. A simple estimate of the total kinetic energy of the differential rotation in the overshoot layer yields  $AE_{\text{diff}} \approx \frac{1}{2}Ad_1\rho(\Delta v_0/2)^2 \approx \frac{1}{8}\rho Ad_1^3 a^2 \approx 7.3 \times 10^{37} \text{ erg}$ . Here  $\rho \approx 0.23 \text{ g cm}^{-3}$  is the mass density and  $\Delta v_0 = ad_1 \approx 8 \times 10^3 \text{ cm s}^{-1}$  is the difference in rotational velocity across the overshoot layer. It follows that  $AE_{\text{diff}}$  is about two orders of magnitude smaller than the total magnetic energy of the dynamo. Therefore differential rotation can provide the energy for the dynamo only if it is very efficiently replenished. In fact, the build-up timescale of  $E_{\text{diff}}$  must be about  $AE_{\text{diff}}/AQ_{\text{diss}} \lesssim 6 \text{ days}$ , if we employ  $AQ_{\text{diss}} \gtrsim 0.04L_\odot$ . Such a rapid conversion of kinetic energy to magnetic energy in the overshoot layer requires in turn an efficient coupling with the convection zone.

*Acknowledgements.* This research was supported by the Netherlands Foundation for Research in Astronomy (NFRA).

## Appendix A: dispersion relation for the mean magnetic field

The boundary conditions for  $B_0$  provide the following relations between the integration constants:

$$e^{-\kappa_1 d_1} A_1 + e^{\kappa_1 d_1} B_1 = 0, \quad (\text{A1})$$

$$\left\{ \frac{ad_1 k_z (\kappa_1 d_1 - 1)}{2\beta_1 \kappa_1} A_1 - \kappa_1 A_2 \right\} e^{-\kappa_1 d_1} + \left\{ \frac{ad_1 k_z (\kappa_1 d_1 + 1)}{2\beta_1 \kappa_1} B_1 + \kappa_1 B_2 \right\} e^{\kappa_1 d_1} = 0, \quad (\text{A2})$$

$$A_2 + B_2 - A_4 - B_4 = 0, \quad (\text{A3})$$

$$A_1 + B_1 - (A_3 + B_3)/f_d = 0, \quad (\text{A4})$$

$$f_d \kappa_1 (A_1 - B_1) - \kappa_2 (A_3 - B_3) + \frac{\alpha}{2\beta_2 \kappa_2 d_2} (A_4 - B_4) = 0, \quad (\text{A5})$$

$$\frac{id_1 k_z}{2\beta_2 \kappa_1} (A_1 - B_1) + f_\beta \kappa_1 (A_2 - B_2) - \kappa_2 (A_4 - B_4) = 0, \quad (\text{A6})$$

$$e^{-\kappa_2 d_2} A_4 + e^{\kappa_2 d_2} B_4 = 0, \quad (\text{A7})$$

$$(k_z + \kappa_2) e^{\kappa_2 d_2} A_3 + (k_z - \kappa_2) e^{-\kappa_2 d_2} B_3 - \frac{\alpha}{2\beta_2} \left\{ 1 + \frac{1 + k_z d_2}{\kappa_2 d_2} \right\} e^{\kappa_2 d_2} A_4 - \frac{\alpha}{2\beta_2} \left\{ 1 - \frac{1 + k_z d_2}{\kappa_2 d_2} \right\} e^{-\kappa_2 d_2} B_4 = 0. \quad (\text{A8})$$

Here  $f_d = d_1/d_2$ . These equations may be represented as an 8 by 8 matrix operating on the integration constants  $A_1, A_2, \dots, B_4$ . The dispersion relation results from equating its determinant to zero.

### Appendix B: expressions for the mean magnetic energy tensor

With ansatz (54), Eqs. (43-44) become

$$(\Lambda + 2\nu_1 - \beta_1 \partial_x^2) \tilde{T}'_\mu = \sum_\nu (aX_{\mu\nu} + \frac{2}{5}\gamma_1 \Gamma_{\mu\nu}) \tilde{T}'_\nu, \quad (\text{B1})$$

$$(\Lambda + 2\nu_2 - \beta_2 \partial_x^2) \tilde{T}'_\mu = \sum_\nu (\alpha \Xi_{\mu\nu} \partial_x + \frac{2}{5}\gamma_2 \Gamma_{\mu\nu}) \tilde{T}'_\nu. \quad (\text{B2})$$

Here the matrices  $\Gamma$ ,  $\mathbf{X}$  and  $\Xi$  are

$$\Gamma = \begin{pmatrix} 1 & 0 & 0 & 2 & 0 & 2 \\ 0 & -1 & 0 & 0 & 0 & 0 \\ 0 & 0 & -1 & 0 & 0 & 0 \\ 2 & 0 & 0 & 1 & 0 & 2 \\ 0 & 0 & 0 & 0 & -1 & 0 \\ 2 & 0 & 0 & 2 & 0 & 1 \end{pmatrix}, \quad \mathbf{X} = \begin{pmatrix} 0 & 0 & 0 & 0 & 0 & 0 \\ 1 & 0 & 0 & 0 & 0 & 0 \\ 0 & 0 & 0 & 0 & 0 & 0 \\ 0 & 2 & 0 & 0 & 0 & 0 \\ 0 & 0 & 1 & 0 & 0 & 0 \\ 0 & 0 & 0 & 0 & 0 & 0 \end{pmatrix}, \quad (\text{B3})$$

$$\Xi = \begin{pmatrix} 0 & 0 & 0 & 0 & 0 & 0 \\ 0 & 0 & -1 & 0 & 0 & 0 \\ 0 & 1 & 0 & 0 & 0 & 0 \\ 0 & 0 & 0 & 0 & -2 & 0 \\ 0 & 0 & 0 & 1 & 0 & -1 \\ 0 & 0 & 0 & 0 & 2 & 0 \end{pmatrix}. \quad (\text{B4})$$

Of these matrices,  $\Gamma$  and  $\Xi$  can be diagonalised simultaneously. Therefore Eq. (B2) is easily solved, but we start with Eq. (B1), from which it readily follows that

$$\tilde{T}'_{xx} - \tilde{T}'_{zz} = C_1 e^{k_1 x} + D_1 e^{-k_1 x}, \quad (\text{B5})$$

$$\tilde{T}'_{xz} = C_3 e^{k_1 x} + D_3 e^{-k_1 x}, \quad (\text{B6})$$

where  $k_1 = \sqrt{(\Lambda + 2\nu_1 + \frac{2}{5}\gamma_1)/\beta_1}$ . Next we solve  $\tilde{T}'_{yz}$ , which is coupled to  $\tilde{T}'_{xz}$  in a resonant manner:

$$\tilde{T}'_{yz} = C_5 e^{k_1 x} + D_5 e^{-k_1 x} - \frac{ax}{2\beta_1 k_1} (C_3 e^{k_1 x} - D_3 e^{-k_1 x}). \quad (\text{B7})$$

The following equation for  $\mathbf{w} = (\tilde{T}'_{xx} + \tilde{T}'_{zz}, \tilde{T}'_{xy}, \tilde{T}'_{yy})$  remains:

$$(\Lambda + \frac{2}{5}\gamma_1 - \beta_1 \partial_x^2) \mathbf{w} = \begin{pmatrix} \frac{8}{5}\gamma_1 & 0 & \frac{8}{5}\gamma_1 \\ a/2 & 0 & 0 \\ \frac{4}{5}\gamma_1 & 2a & \frac{4}{5}\gamma_1 \end{pmatrix} \mathbf{w} + \frac{1}{2}a(\tilde{T}'_{xx} - \tilde{T}'_{zz}) \begin{pmatrix} 0 \\ 1 \\ 0 \end{pmatrix}. \quad (\text{B8})$$

The matrix  $\mathbf{M}$  on the right hand side is transformed into diagonal form  $\mathbf{U}\mathbf{M}\mathbf{U}^{-1}$  by means of a transformation matrix  $\mathbf{U}$ , which is not reproduced here explicitly. Hence the solution of Eq. (B8) may be expressed as

$$\begin{pmatrix} \tilde{T}'_{xx} + \tilde{T}'_{zz} \\ \tilde{T}'_{xy} \\ \tilde{T}'_{yy} \end{pmatrix} = \mathbf{U}^{-1} \begin{pmatrix} w'_2 \\ w'_4 \\ w'_6 \end{pmatrix}. \quad (\text{B9})$$

Here

$$w'_\mu = C_\mu e^{k_\mu x} + D_\mu e^{-k_\mu x} - \frac{aU_{\mu 4}}{2m_\mu} (\tilde{T}'_{xx} - \tilde{T}'_{zz}) \quad (\mu = 2, 4, 6), \quad (\text{B10})$$

and  $m_\mu$  are the eigenvalues of  $\mathbf{M}$ , i.e. the solutions of

$$m_\mu^3 - \frac{24}{25}\gamma_1^2 m_\mu^2 - \frac{8}{5}a^2 \gamma_1 = 0. \quad (\text{B11})$$

The wavenumbers  $k_\mu$  are

$$k_\mu = \sqrt{(\Lambda + 2\nu_1 + \frac{2}{5}\gamma_1 - m_\mu)/\beta_1} \quad (\mu = 2, 4, 6). \quad (\text{B12})$$

The general solution of Eq. (B1) is provided by Eqs. (B5–B7) and (B9).

In region 2 we proceed as follows. We transform  $\Gamma$  and  $\Xi$  to diagonal forms  $\mathbf{S}\Gamma\mathbf{S}^{-1}$  and  $\mathbf{S}\Xi\mathbf{S}^{-1}$  respectively, where  $\mathbf{S}$  is the corresponding transformation matrix (not reproduced here). This provides the following general solution of Eq. (B2):

$$\tilde{T}'_\mu = \sum_\nu (\mathbf{S}^{-1})_{\mu\nu} h_\nu \quad (\mu = xx, xy, \dots, zz; \nu = 7, 8, \dots, 12), \quad (\text{B13})$$

where

$$h_\mu = C_\mu e^{k_{\mu\pm} x} + D_\mu e^{-k_{\mu\pm} x} \quad (\mu = 7, 8, \dots, 12). \quad (\text{B14})$$

The wavenumbers  $k_{\mu\pm}$  are

$$k_{7\pm} = \pm \sqrt{(\Lambda + 2\nu_2 - 2\gamma_2)/\beta_2}, \quad (\text{B15})$$

$$k_{8\pm} = -i \frac{\alpha}{2\beta_2} \pm \sqrt{(\Lambda + 2\nu_2 + \frac{2}{5}\gamma_2)/\beta_2 - \alpha^2/4\beta_2^2}, \quad (\text{B16})$$

$$k_{9\pm} = i \frac{\alpha}{2\beta_2} \pm \sqrt{(\Lambda + 2\nu_2 + \frac{2}{5}\gamma_2)/\beta_2 - \alpha^2/4\beta_2^2}, \quad (\text{B17})$$

$$k_{10\pm} = \pm \sqrt{(\Lambda + 2\nu_2 + \frac{2}{5}\gamma_2)/\beta_2}, \quad (\text{B18})$$

$$k_{11\pm} = -i \frac{\alpha}{\beta_2} \pm \sqrt{(\Lambda + 2\nu_2 + \frac{2}{5}\gamma_2)/\beta_2 - \alpha^2/\beta_2^2}, \quad (\text{B19})$$

$$k_{12\pm} = i \frac{\alpha}{\beta_2} \pm \sqrt{(\Lambda + 2\nu_2 + \frac{2}{5}\gamma_2)/\beta_2 - \alpha^2/\beta_2^2}. \quad (\text{B20})$$

### Appendix C: boundary conditions for the mean magnetic energy tensor

In the solar interior ( $x < -d_1$ ), turbulent diffusivity vanishes, so that  $\beta$  in Eq. (39) assumes the negligible molecular value  $\eta \ll \beta_1$ . There is no  $\alpha$ -effect below the convection zone ( $\alpha = 0$  for  $x < 0$ ). Applying Eq. (47) at  $x = -d_1$ , we find  $\beta_1 \partial_x T_{ij}|_{-d_1} = 0$ , i.e.

$$\partial_x T_\mu = 0 \quad \text{at } x = -d_1 \quad (\mu = xx, xy, \dots, zz). \quad (\text{C1})$$

Consequently, the energy flux across this boundary vanishes:  $\partial_x \epsilon_1|_{-d_1} = 0$ . Continuity of  $\mathbf{T}$  at  $x = 0$  yields

$$T_\mu = T'_\mu \quad \text{at } x = 0 \quad (\mu = xx, xy, \dots, zz). \quad (\text{C2})$$

We apply Eq. (47) at  $x = 0$ , which provides

$$\left. \begin{aligned} \beta_1 \partial_x T_{xx} &= \beta_2 \partial_x T'_{xx} \\ \beta_1 \partial_x T_{xy} &= \beta_2 \partial_x T'_{xy} - \alpha T'_{xz} \\ \beta_1 \partial_x T_{xz} &= \beta_2 \partial_x T'_{xz} + \alpha T'_{xy} \\ \beta_1 \partial_x T_{yy} &= \beta_2 \partial_x T'_{yy} - 2\alpha T'_{yz} \\ \beta_1 \partial_x T_{yz} &= \beta_2 \partial_x T'_{yz} + \alpha(T'_{yy} - T'_{zz}) \\ \beta_1 \partial_x T_{zz} &= \beta_2 \partial_x T'_{zz} + 2\alpha T'_{yz} \end{aligned} \right\} \text{ at } x = 0. \quad (\text{C3})$$

Note that the first, fourth and sixth of these equations together guarantee a continuous energy flux across  $x = 0$ .

At  $x = d_2$ , we assume that the magnetic energy density at the surface is equally distributed among its components  $T_{xx}$ ,  $T_{yy}$  and  $T_{zz}$ . The idea is that due to the reprocessing of the (predominantly azimuthal) field on its way up through the convection zone, the field is small-scale and shows no net preference for any direction at the surface. By the same token, the off-diagonal elements of  $\mathbf{T}$  should then vanish near the surface:

$$\left. \begin{aligned} T'_{xx} &= T'_{yy} = T'_{zz} \\ T'_{xy} &= T'_{xz} = T'_{yz} = 0 \end{aligned} \right\} \text{ at } x = d_2. \quad (\text{C4})$$

For the remaining condition at  $x = d_2$  we refer to the main text (Eq. 49).

## References

- Biskamp, D. 1993, *Nonlinear Magnetohydrodynamics*, Cambridge Monographs on Plasma Physics, Cambridge University Press (Cambridge)
- Brandenburg, A. 1993, in *The Cosmic Dynamo*, IAU-Symposium 157, Kluwer (Dordrecht), p. 111
- Caligari, P., Moreno-Insertis, F., Schüssler, M. 1995, ApJ 441, 886
- Choudhuri, A.R. 1989, Sol. Phys. 123, 21
- Choudhuri, A.R. 1990, ApJ 355, 733
- D'Silva, S., Choudhuri, A.R. 1993, A&A 272, 621
- Galloway, D.J. and Weiss, N.O. 1981, ApJ 243, 945
- Golub, L., Rosner, R., Vaiana, G.S. and Weiss, N.O. 1981, ApJ 377, 309
- Goode, P.R. 1995, in *Fourth Soho Workshop: Helioseismology*, eds. J.T. Hoeksema, V. Domingo, B. Fleck and B. Battrick, ESA SP-376, Vol. 1, p. 121
- Hewitt, J.M., McKenzie, D.P., Weiss, N.O. 1975, J. Fluid Mech. 68, 721
- Hoyng, P. 1987, A&A 171, 357
- Hoyng, P. 1992, in *The Sun, a Laboratory for Astrophysics*, eds. J.T. Schmelz and J.C. Brown, Kluwer (Dordrecht), p. 99
- Knobloch, E. 1978, ApJ 220, 330
- Krause, F. and Rädler, K.-H. 1980, *Mean Field Magnetohydrodynamics and Dynamo Theory*, Pergamon Press (Oxford)
- Kuperus, M., Ionson, J.A. and Spicer, D.S. 1981, ARA&A 19, 7
- Moffatt, H.K. 1978, *Magnetic Field Generation in Electrically Conducting Fluids*, Cambridge University Press
- Moreno-Insertis F., Schüssler, M. and Ferriz-Mas, A. 1992, A&A 264, 686
- Nordlund, A., Brandenburg, A., Jennings, R.L., Rieutord, M., Ruokolainen, J., Stein, R.F. and Tuominen, I. 1992, ApJ 392, 647

- Ossendrijver, A.J.H., Hoyng, P. and Schmitt, D. 1996, A&A 313, 938
- Parker, E.N. 1993, ApJ 408, 707
- Spiegel, E.A. and Weiss, N.O. 1980, Nat 287, 616
- Schüssler, M., Caligari, P., Ferriz-Mas, A. and Moreno-Insertis, F. 1994, A&A 281, L69
- Stix, M. 1989, *The Sun, an Introduction*, Springer-Verlag (Berlin)
- Van Ballegooijen, A.A. 1982, A&A 113, 99
- Van Geffen, J.H.G.M. and Hoyng, P. 1993, Geophys. Astrophys. Fluid Dynamics 71, 187
- Van Geffen, J.H.G.M. 1993a, Geophys. Astrophys. Fluid Dynamics 71, 223
- Van Geffen, J.H.G.M. 1993b, A&A 274, 534
- Van Kampen, N.G. 1992, *Stochastic processes in physics and chemistry*, North Holland (Amsterdam)
- Withbroe, G.C. and Noyes, R.W. 1977, ARA&A 15, 363
- Zwaan, C. 1978, Sol. Phys. 60, 213